Geoscience Frontiers 8 (2017) 125–135

HOSTED BY

Contents lists available at ScienceDirect

China University of Geosciences (Beijing)

Geoscience Frontiers

journal homepage: www.elsevier.com/locate/gsf

Research paper

Supracrustal suite of the Precambrian crystalline crust in the Ghor Province of Central Afghanistan

Gediminas Motuza [a,*], Saulius Šliaupa [b]

[a] Department of Geology and Mineralogy, Vilnius University, M.K.Čiurlionio 21/27, LT-03101 Vilnius, Lithuania
[b] Nature Research Centre, Akademijos 2, LT- 08412 Vilnius, Lithuania

ARTICLE INFO

Article history:
Received 8 January 2015
Received in revised form
4 December 2015
Accepted 29 December 2015
Available online 3 February 2016

Keywords:
Afghanistan
Tajik block
Proterozoic rock units
Continental arc
Back-arc basin

ABSTRACT

The Proterozoic pre-Ediacaran metamorphic basement of the southern Tajik (North Afghanistan) continental block and the adjacent Band-e-Bayan zone is exposed in the Ghor Province of Central Afghanistan. It is predominantly composed of the EW-striking supracrustal succession consisting of interbedded felsic schists and gneisses (metapsammites), amphibolites (metabasalts), calcite and dolomite marbles. The metamorphic facies changes from greenschist in the Band-e-Bayan zone to amphibolite facies in the Tajik block. The supracrustal rocks of the Band-e-Bayan zone and Tajik block possess common features suggesting that the former represents a tectonized part of the latter. The geochemical characteristics of metapsammites indicate derivation of the clastic material from a continental arc and, partly from a passive continental margin, whereas the composition of metabasalts suggests their possible formation in a continental rift basin. The tectonic setting of supracrustal unit could be interpreted as a back-arc type basin. We presume that the Tajik microcontinent split off the Gondwana supercontinent along an ancient rift zone during the late Paleozoic.

1. Introduction

The Afghanistan segment of the Alpine-Himalayan orogenic system shows a complex Permian–Quaternary history of successive amalgamation of different microcontinental blocks to the Asian continent (Şengör and Natal'in, 1996; Klett et al., 2006; Kalvoda and Bábek, 2010). The available information on the crystalline crust of these continental blocks in Afghanistan is scarce. The central part of Afghanistan was first systematically mapped by the German Geological Mission in the 60s, compiling a geological map at the scale of 1:500,000 where the Precambrian metamorphic rocks underlying the sedimentary cover were identified (Wittekindt and Weppert, 1973). The Soviet geological mission initiated more detailed geological exploration and mapping activities in the sixties and seventies. The central part of Afghanistan was covered by mapping at a scale of 1:200,000 with some areas at 1:50,000 and 1:10,000 scales (Dronov et al., 1972, 1973). The metamorphosed Precambrian basement rocks mostly overlain by sediments were studied in significant detail. The results have been published in several compilations (Abdullah and Chmyriov, 1977, 1980).

Since 1979, field geological studies have ceased, and the main activities were focused on the systematization of the available information, such as the compilation of a 1:2,000,000 geological map published in 1995 by the United Nations Economic and Social Commission for Asia and the Pacific (ESCAP) in cooperation with the Department of Mines and Geological Survey of Afghanistan (Atlas of Mineral Resources of the ESCAP Region Series, 1995).

The United States Geological Survey (USGS) in co-operation with the Afghanistan Geological Survey carried out an assessment of the mineral resources of Afghanistan based on the compilation and reinterpretation of existing geological materials (Peters et al., 2007) and prepared a digitized geological map of Afghanistan (Doebrich and Wahl, 2006). This map is based on the one published by Abdullah and Chmyriov (1980), keeping original geological boundaries.

The Tajik (North Afghanistan) block represents the largest lithotectonic domain of Afghan continental collage. The rocks in the crystalline basement are mainly of Precambrian age and are exposed in some areas, while most of the territory is buried under thick

* Corresponding author. Tel.: +37062077932.
E-mail addresses: gediminas.motuza@gf.vu.lt (G. Motuza), sliaupa@geo.lt (S. Šliaupa).
Peer-review under responsibility of China University of Geosciences (Beijing).

http://dx.doi.org/10.1016/j.gsf.2015.12.011

package of sedimentary cover. There are no detailed studies as yet in relation to the primary composition and tectonic environment of formation of the basement rocks. Furthermore, the southern margin of the Tajik block is embroidered by more than 700 km long highly deformed Band-e-Bayan zone, the origin of which is debated.

The metamorphic basement rocks of the southern margin of the Tajik block and the Band-e-Bayan zone are exposed in the middle part of the Ghor Province of central Afghanistan. Geochemical and petrological studies with a view to understand the evolution of the Proterozoic metamorphic succession were undertaken and the results presented in this paper are based on field observations in the Ghor Province performed in 2008 and 2011 (Fig. 1). The study area was confined to the catchment of the Hari Rod River and its tributaries, from the western border near Jam to the eastern border of the Ghor Province. One hundred and thirty one sites were inspected and sampled, including 48 locations of Precambrian metamorphic rocks (Fig. 2).

2. Geological setting

The study area is located in central Afghanistan at the junction of the Tajik (North Afghanistan) and Farah Rod (also referred to as the Middle Afghanistan) blocks separated by the Band-e-Bayan zone (Fig. 1).

The Band-e-Bayan zone is an elongated narrow crustal block oriented in a W–E direction, bounded on the North by the major Herat Fault (also referred to as the Hari Rod), and the southern border limited by the distribution of the Pre-Mesozoic rocks, which are absent in the south. The nature of the zone has not been well investigated and could be considered as (1) a tectonized margin of the Tajik block, (2) an uplifted northern margin of the Farah Rod block, and (3) an exotic block.

The Precambrian metamorphic rocks are exposed along the southern margin of the Tajik block and in the Band-e-Bayan zone (Fig. 2).

In the Ghor portion of the Tajik block, the metamorphic basement is covered by sedimentary sequences ranging in age from Carboniferous to Quaternary. In the Band-e-Bayan zone the metamorphic basement is covered by sediments ranging in age from the Ediacaran (Vendian) to Quaternary. Most of the Paleozoic paleogeographic reconstructions suggest a peri-Gondwana affinity for the Tajik block (von Raumer et al., 2002; Klett et al., 2006; Kalvoda and Bábek, 2010).

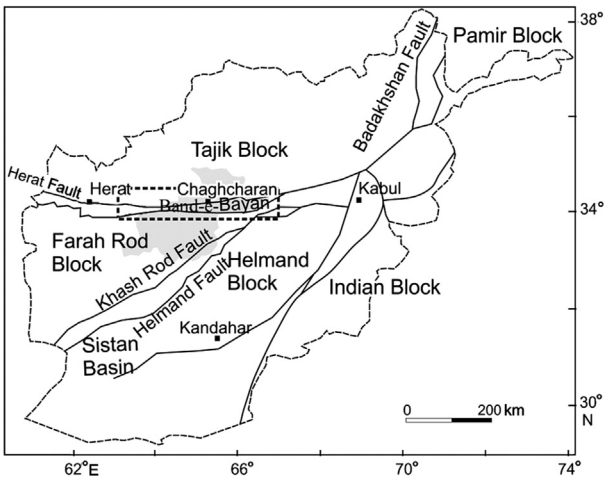

Figure 1. Generalized tectonic framework of Afghanistan (after Peters et al., 2007). Shaded area marks the Ghor Province.

The nature of the Farah Rod block is not well understood. It is composed of a very thick sedimentary pile that can be viewed as an accretionary complex of Mesozoic and Tertiary age. There are no exposures of the Paleozoic sedimentary sequences and the underlying metamorphic basement.

3. Age of the metamorphic basement

No isotope age data are available for the metamorphic rocks from the Tajik block and Band-e-Bayan zone. The basement of the Band-e-Bayan zone is locally overlain by Ediacaran and Cambrian unmetamorphosed sediments which suggesting its Precambrian age (Dronov et al., 1973). Geochronology of similar basement rocks exposed in other crustal blocks of Afghanistan show Paleo- and Mesoproterozoic (Nadimi, 2007) or Neoproterozoic (Saki, 2010) ages.

In previous studies, the metamorphic rocks of the Ghor Province were subdivided into two lithological units: (1) a mafic metavolcanic unit with subordinate metasediments and (2) a metasedimentary unit with rare metavolcanics (Dronov et al., 1973). They were tentatively identified as Mesoproterozoic based on low grade (predominantly greenschist facies) metamorphism (Abdullah and Chmyriov, 1977, 1980). The stratigraphic subdivision of metamorphic rocks is represented slightly differently on the map compiled by the USGS team (Fig. 2). The sequence outcropping in the westernmost part of the Ghor Province is characterized by a higher metamorphic grade (amphibolites facies) and was accordingly attributed to the Paleoproterozoic (unit X*gn*) comprising gneisses, migmatites, amphibolites, quartzites, and marble, while the metamorphic sequence distributed further east was attributed to the Mesoproterozoic (units Y*m* and Y*vl*). The unit Y*m* comprises undifferentiated metamorphic rocks including “greenschist, gneiss, quartzite, marble, amphibolite (metavolcanic lava and sedimentary rocks)”, whereas unit Y*vl* is characterised as “metavolcanic lava and sedimentary rocks” (Doebrich and Wahl, 2006).

4. Petrography

Based on our observations, three lithological groups are defined in the crystalline basement of the Ghor Province, i.e. felsic metasedimentary gneisses, greenschists (primary basic metavolcanics), and marbles. The rocks of all groups are interbedded and form common sequence. Felsic gneisses are predominant both in the Band-e-Bayan zone and the Tajik block. Marbles and greenschists are more common in the Band-e-Bayan zone, while in the north they were observed only in one locality (Loc. G93; Fig. 3C).

Felsic gneisses are subdivided into two subgroups: (1) muscovite gneisses and (2) biotite gneisses. Muscovite gneisses occur in the Band-e-Bayan zone, south of the Herat Fault, while biotite gneisses are distributed to the north of the Herat Fault, along the southern margin of the Tajik block.

The basement rocks of the Band-e-Bayan zone are metamorphosed under greenschist facies as indicated by characteristic mineral assemblage, including muscovite, epidote, chlorite, actinolite. The grade of metamorphism increases to the north and west, reaching amphibolite facies in the Tajik block. The presence of metatexite migmatites suggests partial melting in the western part of the study area. The sequence is folded to predominantly isoclinal folds, striking generally in an E–W direction, parallel to the southern margin of the Tajik block and the Band-e-Bayan zone. The lithologies strike in the same direction and can be traced to tens of kilometres (Fig. 3).

The intrusive rocks that might be attributed to Precambrian are scarce. A few small bodies of intrusive rocks affected by metamorphism were observed in the Tajik block north of the Herat Fault

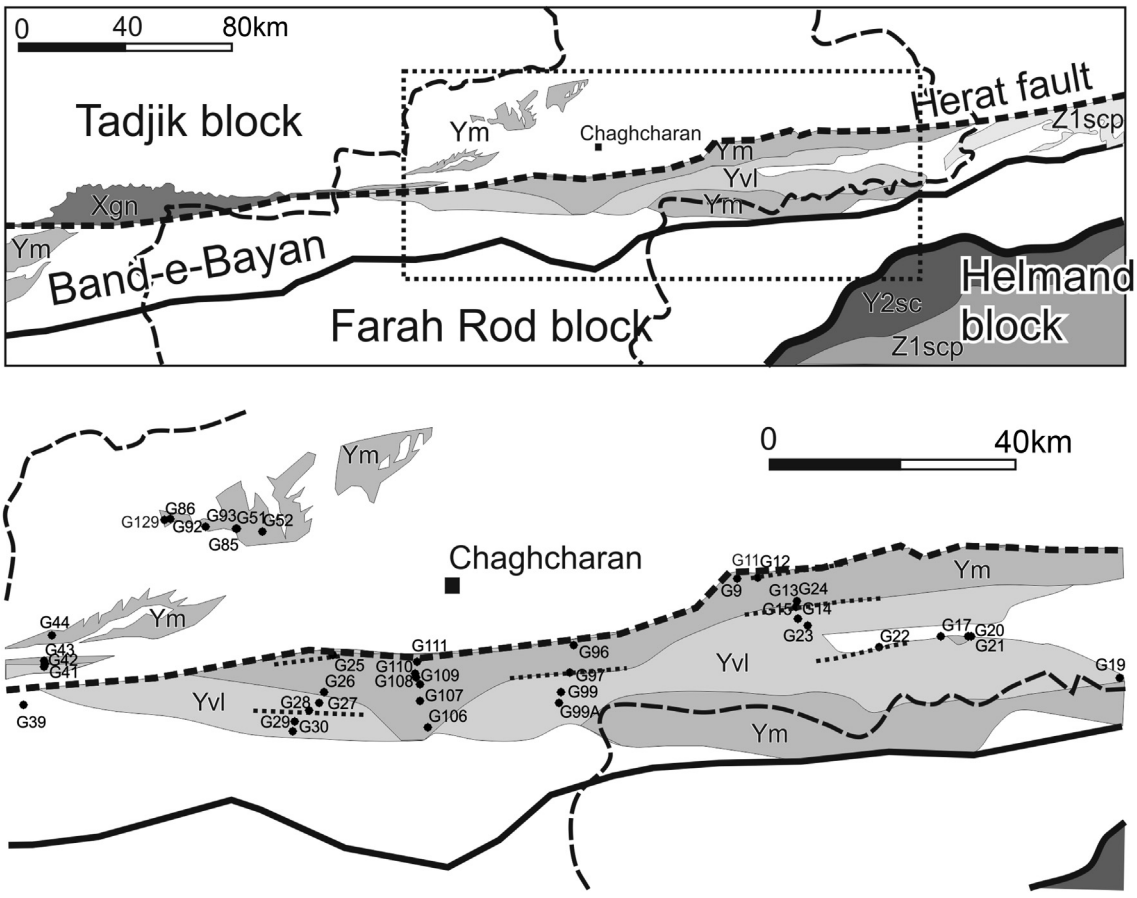

Figure 2. Proterozoic units of central Afghanistan (modified from Doebrich and Wahl, 2006; Peters et al., 2007). Paleoproterozoic: X*gn*—two-mica, biotite, biotite-amphibole, garnet-biotite, and plagioclase gneisses; migmatite, quartzite, marble, amphibolite. Mesoproterozoic: Y*vl*—metavolcanic lava and marbles; Y*m*—greenschist, gneiss, quartzite, marble, amphibolite; Y_2sc—albite-sericite-quartz and sericite-plagioclase-quartz schists, with amphibolite beds and lenses. Neoproterozoic: Z_1scp—greenschist and phyllite schist, sandstone subordinated marble, chert and metavolcanic rocks. Dotted lines show extent of fixed marble lenses. Bold line marks southern boundary of Band-e-Bayan zone. Observation sites are indicated. Hatchet lines indicate border of Ghor province.

including two hornblende gabbro (Loc. G86; G129) and a layered serpentinite sequence, roughly 100 m thick (Loc. G52).

4.1. Felsic gneisses

Muscovite gneisses consist of quartz, plagioclase, microcline, muscovite, calcite, and biotite. The accessory minerals are zircon (usually rounded, likely detrital), apatite, opaque and tourmaline. The content of the felsic minerals is variable, particularly of quartz which composes up to 70–75% of the volume of the rock. The content of muscovite is in the range of 10–20%, while biotite is minor. Calcite is commonly present up to a few percent, but in some varieties reaches up to 30–40% (Loc. G13A; G109; G116) (Fig. 3A, B). Calcite is evenly distributed in the rock, and presumably is the primary rock forming component. Such rocks form particular layers which can be followed for long distances as regular part of supracrustal sequence. Gneisses containing actinolite, epidote, and chlorite together constituting up to 15–20%, carry accessory titanite. The texture is very fine (<0.3 mm) to fine (0.3–1 mm) grained lepidogranoblastic, and the structure is gneissic or schistose, often banded.

The subgroup of biotite gneisses comprises biotite-feldspar-quartz gneiss often containing cordierite and muscovite with accessory tourmaline (Loc. G43A); epidote-actinolite-feldspar-quartz gneiss with chlorite and titanite (Loc. G92); biotite-garnet-feldspar-quartz gneiss with sillimanite, kyanite (Loc. G52A). The rocks are fine grained (size 0.1–0.3 mm, some place up to 0.5 mm). Garnet occurs as rounded blasts up to 0.5 mm in diameter (Fig. 4C). Sillimanite occurs as fine needle-like inclusions in garnet and elongated aggregates up to 1.5 mm in length. Kyanite appears in elongated crystals up to 0.7 mm long (Fig. 4C). Cordierite amounts to 10%, in the form of xenomorphic blasts up to 0.3 mm concentrated in particular bands (Fig. 4D). Structure is gneissic, and faintly banded due to irregular distribution of biotite and plagioclase.

Petrological features of felsic gneisses suggest psammitic protolith. This is also indicated by a regularly fine grained texture, often banded structure, presumably reflecting primary bedding. Relics of psammitic texture have been noticed in the form of regenerated primary abraded clasts of quartz (Fig. 4B).

4.2. Marbles

Marbles form layered sequences of tens to hundreds of meters thick interbedded with felsic gneisses and greenschists. They are composed mainly of calcite, rarely dolomite, and are off white, gray, yellow, and black color. The rocks are predominantly fine grained.

4.3. Greenschists

The greenschist unit consists predominantly of chlorite-epidote-actinolite-plagioclase schists. Content of mafic minerals vary, but

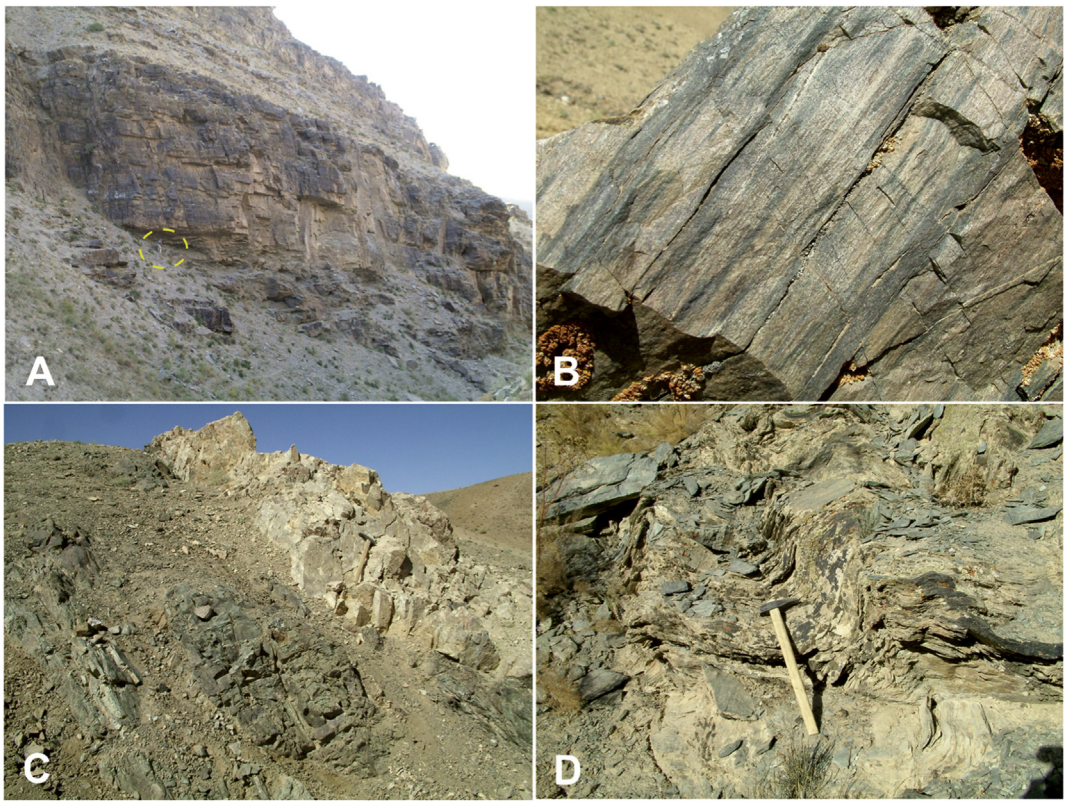

Figure 3. The outcrops of Precambrian supracrustals in Ghor Province investigated in this study. (A) Muscovite gneisses (Loc. G109), the dotted circle is the man for scale; (B) biotite gneiss (Loc. G92); (C) contact between greenschist and marble (Loc. G93); (D) folded greenschist (Loc. G110).

mainly is about 10–20% of each. Plagioclase comprises 40% of rock volume. The size of crystals is 0.2–0.5 mm, rarely 1–1.5 mm. Lensoid aggregates of mm size are often observed, which likely represent primary phenocrysts, and relic porphyry texture (Fig. 4E, F). Typical accessory mineral is leucoxene which occurs as irregular elongated earthy aggregates up to a few mm long.

5. Geochemistry

5.1. Methods and data

Chemical composition was analyzed in 20 whole rock samples of felsic gneisses and 9 samples of greenschists at Acme Laboratories, Canada. Abundances of the major oxides and trace elements, including REE were determined by ICP-MS following a lithium metaborate/tetrabortate fusion and nitric acid digestion of a 0.2 g sample. The samples were taken from natural outcrops, in few cases from road cuts, and mostly from fresh and unaltered rocks.

The LOI for gneisses varies from 0.8 to 5.2 wt.%, except for the carbonate-rich varieties where it is up to 10.8 wt.%.

LOI of greenschists varies from 1.8 to 5.9 wt.% (Table 1) suggesting that some samples might be altered by low degree weathering. Metamorphism of greenschist and partly amphibolite facies also might have affected the primary chemical composition of rocks, although the alteration is low. On spider diagrams, only a few samples show difference in elemental concentrations. In particular, sample G19 contains lower concentrations of Rb, Ba, K, and G25 shows higher content of Pb (Fig. 10). Relative immobility of elements is indicated also by linear correlation between Zr and immobile elements, including REE (Dampare et al., 2007). The contents of immobile HFSE and REE group elements were mainly used for the geochemical characterization of the rocks.

5.2. Felsic gneisses

SiO_2 content of felsic gneisses is in the range of 57–86 wt.% and shows inverse correlation with Al_2O_3 (6.1–22.6 wt.%) (Table 2), which is a common trend of clastic sediments. Muscovite gneisses, in comparison to biotite gneisses, show higher average SiO_2, K_2O, Th, Hf, Zr, Nb, Co, and LREE. Biotite gneisses are relatively enriched in FeO^T, MgO, Sc, V, and Ni. MgO and FeO^T show negative statistical correlation with silica content.

Primary calcite bearing gneisses (samples G13A, G109) fall out of this correlation trend, showing low content of Al_2O_3 (1.7–2.8 wt.%) and high amount of CaO (12.4–12.7 wt.%) and total carbon (2.8–2.9 wt.%), while most of the samples have CaO content in the range of 0.2–2.4 wt.%. Samples G92, G92-1, G116B represent a transitional group (CaO = 4.4–8.7 wt.%).

The ratios of major elements K_2O/Na_2O vs. SiO_2/Al_2O_3 (Wimmenauer, 1984) suggest that the protolith rocks of felsic gneisses were sandstones with admixture of silty and pelitic material, and might be classified as greywackes (predominantly) and arkoses (Fig. 5).

5.3. Greenschists

On the TAS classification diagram, most of the greenschists plot in the field of basalt and picrobasalt, whereas some points cluster in the fields of basaltic trachyandesites (Fig. 6A). Alkalinity is mainly due to Na_2O content (2.2–5.78 wt.%) which is always higher as K_2O (0.08–1.93 wt.%) (Table 1). The alkalinity of rocks is confirmed by classification plot Zr/Ti vs. Nb/Y using immobile elements (Fig. 6B). CaO content varies between 2 and 11 wt.%. TiO_2 content is $>$ 1.5 wt.%, what is typical for continental tholeiites and alkali basalts.

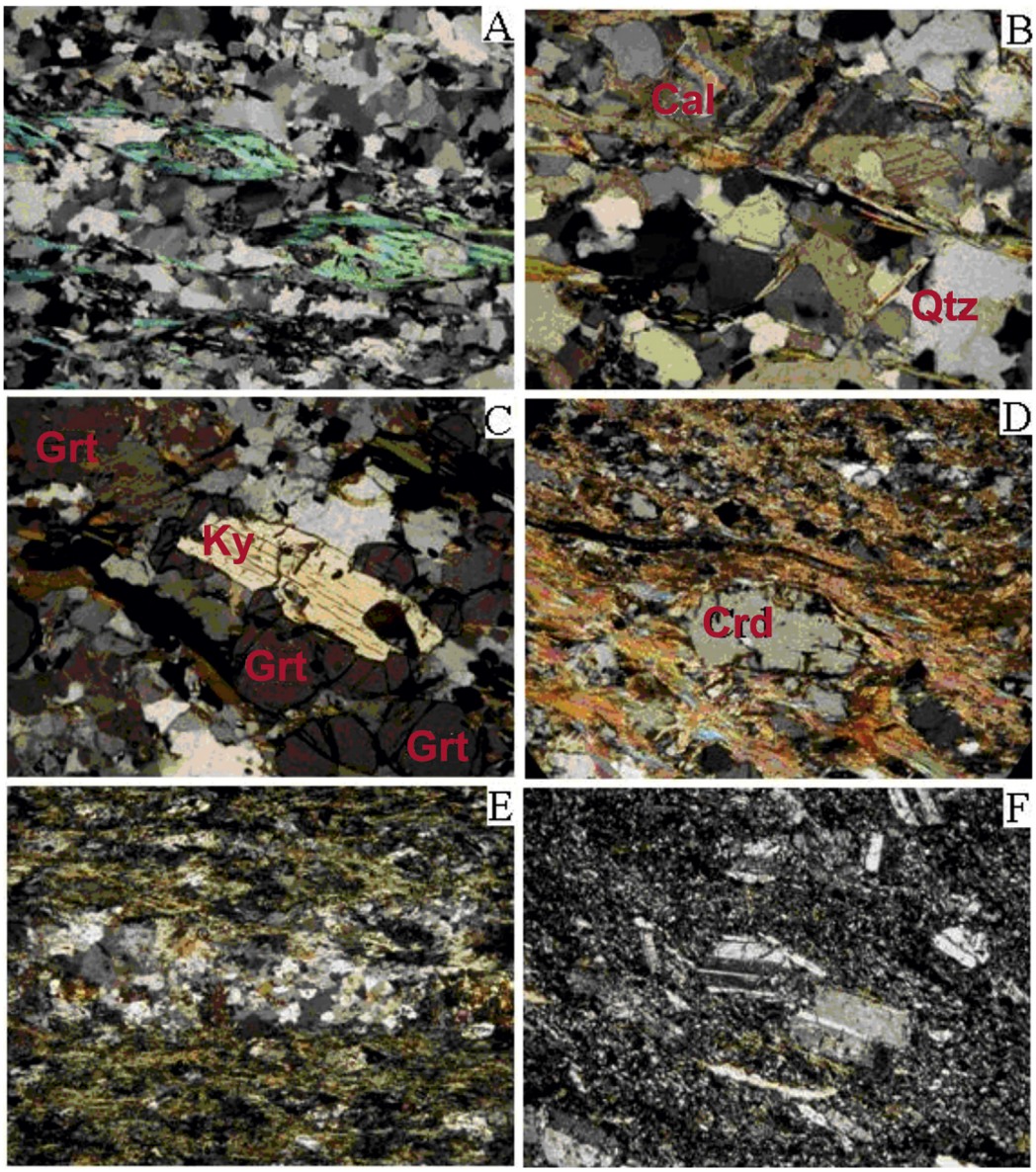

Figure 4. Photomicrographs (crossed nicols) of the metamorphic supracrustals of the Ghor Province. (A) Muscovite-feldspar-quartz gneiss (Loc. G9); (B) calcite bearing muscovite-feldspar-quartz gneiss (Loc. G13); (C) kyanite-biotite-garnet-feldspar-quartz gneiss (Loc. G52A); (D) cordierite-biotite-feldspar-quartz gneiss (Loc. 43A); (E) epidote-chlorite plagioclase schist – metaporphyrite with deformed relic plagioclase phenocryst in the centre (Loc. G23); (F) chlorite-plagioclase schist – metaporphyrite with relic plagioclase phenocrysts (Loc. G30). Length of the base in A, B, E, and F is 3 mm, in C and D is 1.5 mm.

6. Discussion

6.1. Provenance

The provenance of clastic material of the Precambrian metasedimentary rocks of Ghor Province was evaluated based on geochemical data, using various diagrams. The Th vs. Sc plot indicates an acidic and intermediate provenance for muscovite gneisses, while the clastic material of biotite gneisses is derived from a more basic source (Fig. 7A).

The Hf vs. La/Th plot indicates that clastic material of biotite gneisses and a part of muscovite gneisses were derived from an acidic volcanic arc source, but the rest of muscovite gneisses consist of material sourced from a passive continental margin (Fig. 7C). This conclusion is supported by the affinity of REE content to the average of the upper continental crust (Fig. 8). It is remarkable that despite the wide geographic scattering of the samples, no discernable differences are recognized on the REE plot, which is typical for continentally sourced sediments.

The protolith of greenschists is classified as sub-alkaline sodic basalt, as also indicated by geochemical data and relict porphyry texture.

6.2. Tectonic setting

The tectonic setting of formation of the sedimentary rocks was estimated by various diagrams (Bhatia, 1983; Bhatia and Crook, 1986), and here we present plots in the La-Th-Sc ternary diagram (Fig. 7B). The plots mostly suggest a continental arc tectonic setting. The same environment together with the passive continental margin was estimated as provenance for the clastic material. This is

Table 1
Chemical composition of greenschists of the Ghor Province (the major oxides in wt.%, trace elements in ppm).

Samples	G17	G19	G23	G23A	G27	G29	G30	G41
SiO_2	44.51	46.48	47.66	41.48	51.06	42.39	51	52.01
TiO_2	2.52	1.86	2.01	4	1.65	3.33	2.55	1.5
Al_2O_3	14.62	18.45	13.09	14.59	17.38	13.57	17.06	17.08
FeO^T	15.34	11.16	11.77	14.67	9.8	18.18	9.67	8.36
MnO	0.21	0.14	0.2	0.22	0.17	0.11	0.07	0.08
MgO	6.4	5.88	10.17	7.07	3.96	5.69	6.35	4.5
CaO	9.55	7.37	6.76	11.31	6.84	4.68	2.14	7.68
Na_2O	2.35	3.67	3.92	2.2	5.04	4.04	5.78	4.15
K_2O	0.66	0.08	0.54	0.29	1.00	0.90	0.61	1.93
P_2O_5	0.33	0.27	0.26	0.49	0.31	0.92	0.59	0.59
Cr_2O_3	0.004	0.003	0.071	0.005	0.014	<0.002	0.007	0.008
LOI	3.2	4.4	3.2	3.2	2.5	5.9	3.9	1.8
Total	99.7	99.77	99.71	99.56	99.74	99.73	99.74	99.7
Cr	27.4	20.5	485.8	34.2	95.8	<13.7	47.9	54.7
Sc	31	32	33	32	18	27	18	19
V	325	255	268	338	152	180	124	177
Co	55	37.9	54.7	51.3	45.1	55.6	26.6	30.7
Ni	38.2	16.1	132.5	62.1	31.5	7	41.8	19.1
Cu	125.9	9.4	47.5	225.4	38.5	18.2	55.4	9.6
Zn	81	69	50	92	103	204	58	23
Ga	22.4	19.3	15.5	25.7	21.7	28.4	23	19.1
Rb	20.3	1.3	13.5	9.5	28.8	11.1	8.8	76.5
Sr	360.2	275.6	229.5	1096.1	330.5	79.2	147.1	651.2
Y	29	31.5	18.9	38	29.8	51	33.6	29.4
Zr	181.7	144.6	139.4	307.3	206.4	377.6	351.2	245.8
Nb	28.8	20.1	22.1	52.5	28.9	33.7	42.9	27.5
Cs	2.2	<0.1	1.3	0.6	2.2	0.6	0.3	1.9
Ba	156	42	90	74	412	109	227	417
La	25	19.9	19.5	45.3	28.8	19.8	38.2	50
Ce	53.4	40.6	39.5	94.5	57.4	44.9	78.6	89.9
Pr	7.21	5.38	5.36	12.55	7.5	6.4	10.67	10.82
Nd	30.3	22.8	22	52.9	31.4	29.1	44.3	41.1
Sm	6.16	5.09	4.63	9.75	6.31	7.12	8.88	6.56
Eu	2.02	1.76	1.52	2.95	1.96	2.33	2.77	1.85
Gd	6.26	5.61	4.59	9.09	6.45	8.89	8.5	5.88
Tb	1.02	0.93	0.71	1.39	1.06	1.57	1.3	0.93
Dy	5.79	5.6	3.96	7.56	5.62	9.11	6.65	5.03
Ho	1.12	1.22	0.78	1.38	1.11	1.89	1.24	1.02
Er	2.89	3.21	1.91	3.75	2.96	5.2	3.36	2.75
Tm	0.41	0.49	0.27	0.52	0.42	0.78	0.46	0.44
Yb	2.54	2.96	1.67	3.11	2.49	4.65	2.76	2.68
Lu	0.36	0.43	0.22	0.44	0.35	0.67	0.4	0.4
Hf	4.7	3.9	3.9	8	5.9	9.6	9.1	6.4
Ta	1.8	1.1	1.2	3.4	1.6	1.9	2.5	1.4
Pb	1.5	0.7	1.8	1.7	27.9	4.4	0.5	1.9
Th	2.9	2.6	2.3	5.7	3.7	3.1	5.4	7.4
U	0.9	0.4	0.6	0.8	0.8	0.9	1.6	1.9
W	0.6	<0.5	<0.5	0.6	114.3	41.8	<0.5	<0.5
Mo	0.2	0.2	<0.1	0.2	0.7	1.5	0.3	0.3
Sn	2	1	1	3	2	3	3	2
Be	1	<1	1	2	1	2	2	1

an indication that the sedimentation area was in the vicinity of both these tectonic domains.

The Nb/Ta and Zr/Hf ratios of 17.6 and 36.3, respectively (Sun and McDonough, 1989; Dampare et al., 2007) are considered as characteristic for mantle derived magmas, and the average values of Ghor metabasalts (17.6 and 37.4) are close to these values suggesting formation from mantle-derived magmas. The chondrite normalized REE pattern is characterized by a steep slope both for LREE and HREE, characterized by average La/Lu ratio of 79, implying a deep (probably garnet lherzolite) mantle source (Murphy, 2007). This is confirmed by the low average Th/Nb ratio of 0.13. This value is close to the average value of the depleted asthenosphere (ca. 0.05), indicating low input of sedimentary component (Dampare et al., 2007).

On the spider diagrams normalized to N-MORB, a strong enrichment in incompatible elements is evident, but is less pronounced when normalized by E-MORB (not shown). These data do not attest to mid-ocean ridge tectonic setting.

Spider diagrams normalized to primitive mantle demonstrate enrichment in incompatible elements characteristic of subduction-related environment, but do not reveal typical negative Nb, and Zr anomalies, which makes such a tectonic setting less plausible (Fig. 9). This presumption is supported by the Th/Yb vs. Nb/Yb plot, where the Ghor samples are confined to the non-arc mantle array (Fig. 10D) and indicate an insignificant contamination by crustal material or modification by subduction related metasomatism (Pearce and Peate, 1995; Dampare et al., 2007). Notably volcanic rocks of intermediate and acidic composition, usually predominant in subduction related volcanic areas, are missing in the study area.

On the diagrams Zr/Y vs. Zr and Zr-Nb-Y the samples of metabasalts are clustered in the fields of within-plate setting (Fig. 10). The REE abundance diagram normalized to ocean island basalts (OIB) shows a close affinity to the rocks of this tectonic setting (Fig. 9B).

Nevertheless, an oceanic within-plate setting is not in concert with carbonates and sandstones which are interbedded with the

Table 2
Chemical composition of felsic gneisses of the Ghor Province (the major oxides in wt.%, trace elements in ppm).

Samples	G9-1	G9-1A	G9-2	G13A	G20	G26	G43A	G52A	G92	G92-1	G96	G96-1	G96-2	G106	G108	G109	G116	G117	G118	G130
SiO_2	85.75	85.77	68.19	70.47	74.82	67.44	66.82	64.99	70.38	65.2	80.25	72.84	68.17	70.65	70.61	73.44	66.00	57.48	60.14	78.69
TiO_2	0.36	0.37	0.73	0.22	0.65	0.75	0.7	0.9	0.47	0.46	0.49	0.64	0.7	0.61	0.63	0.13	0.50	2.09	0.75	0.64
Al_2O_3	6.05	6.96	10.7	2.82	10.08	15.32	14.45	15.63	10.98	9.93	9.19	12.42	14.5	12.74	13.9	1.7	10.56	19.31	16.69	10.17
FeO^T	2.01	1.62	5.59	1.17	2.41	4.42	5.75	7.02	4.66	6.38	1.88	4.42	5.76	3.62	4.34	0.43	3.91	10.17	7.05	3.38
MnO	0.03	0.02	0.07	0.04	0.04	0.05	0.07	0.11	0.11	0.25	<0.01	0.01	0.1	0.05	0.05	0.08	0.10	<0.01	0.05	0.05
MgO	0.41	0.34	0.9	0.51	1.05	2.37	2.83	2.97	2.16	2.57	0.29	0.59	1.02	1.03	1.59	0.26	3.19	0.52	3.99	1.11
CaO	0.69	0.23	2.36	12.76	2.23	0.33	1.88	1.76	4.44	8.7	0.28	0.48	0.31	2.04	0.45	12.41	5.03	0.69	1.10	0.82
Na_2O	1.43	2.03	0.59	0.12	2.89	2.86	2.55	2.15	3.41	2.83	2.34	2.68	2.43	0.39	2.84	0.12	3.63	0.63	3.40	1.04
K_2O	1.66	1.61	3.34	0.94	2.36	3.54	2.92	3.15	1.29	1.14	1.76	2.19	2.72	3.33	2.38	0.51	0.66	5.22	2.67	2.44
P_2O_5	0.07	0.07	0.07	0.04	0.08	0.11	0.18	0.22	0.11	0.14	0.08	0.22	0.2	0.17	0.16	0.03	0.13	0.37	0.17	0.05
Cr_2O_3	0.004	0.004	0.008	0.002	0.007	0.01	0.012	0.051	0.018	0.029	0.006	0.011	0.011	0.01	0.01	0.004	0.006	0.006	0.015	0.007
LOI	1.4	0.9	7.3	10.8	3.1	2.6	1.6	0.8	1.8	2.3	3.3	3.3	3.9	5.2	2.9	10.7	6.1	3.3	3.8	1.5
Total	99.9	99.88	99.83	99.91	99.72	99.78	99.79	99.71	99.82	99.88	99.85	99.77	99.86	99.8	99.89	99.85	99.83	99.83	99.83	99.9
Cr	27.4	27.4	54.7	13.7	47.9	68.4	82.1	348.9	123.2	198.4	41.1	75.3	75.3	68.4	68.4	27.4	41.1	41.1	102.6	47.9
Sc	4	4	9	2	6	11	14	18	14	13	6	13	13	11	10	1	4	13	16	8
V	35	32	98	21	47	77	100	142	102	96	46	83	87	77	78	<8	31	136	118	65
Co	3.5	2.4	16.4	2	40.1	5.7	15.1	13.4	9.3	18.5	1	3.6	13.1	55.9	43.5	55.9	10.2	6.8	17.3	7.2
Ni	6.8	2.3	50.3	3.4	7.4	16.3	39.2	32.9	26.1	45.9	1.2	16.8	32	23	21.8	2.5	21.4	12.6	48.3	15.1
Cu	4.8	1.2	34.5	3	25.6	6.1	14.1	61	12.7	5.7	2.5	13.9	25.7	7.1	19.7	14	11.5	1.1	26.3	2.6
Zn	29	7	54	43	26	40	79	401	43	23	2	75	75	102	58	5	72	30	78	38
Ga	7.4	7.1	16.7	3.4	13.8	19.8	17.3	17.5	11.1	10.8	10.6	13.7	16.3	16	16.5	1.8	10.5	26.0	21.8	10.2
Rb	44	48	114.6	29	82.6	121.9	103.6	81.5	20.9	23.7	56.9	66.7	88	96.3	86.5	13.9	21.2	159.5	94.1	78.3
Sr	61.6	48.1	70.4	313.3	126	38.7	150.9	253.2	238.7	180.3	98.7	88.6	99.9	59.4	76.7	141.9	369.9	80.1	104.4	197.3
Y	14.1	12.6	32.8	7.6	20.7	29	27.3	34.8	23.7	20.1	16.4	26.6	27.5	24.3	21.5	6.6	24.0	24.7	22.8	20.2
Zr	316.2	381.3	207.3	202.1	509.3	402.1	188.5	238.5	107.7	90.7	260.5	247.5	204.4	185.9	202.6	131.1	364.8	387.0	138.1	263.5
Nb	8.8	9.7	25.6	4.2	16.2	15.8	10.7	16	5.9	4.7	8.6	10.4	11.4	10.6	10	2.7	10.1	55.0	13.3	11.1
Cs	1.1	1.1	5.1	0.8	6.3	3.5	4.1	0.5	1.7	2.1	3.6	8.3	3.7	5.4	5.3	0.4	0.7	9.6	2.7	1.3
Ba	506	530	684	206	957	772	720	704	269	307	440	935	637	775	375	142	232	391	481	774
La	18.3	17.1	30.8	8.5	29.1	45.4	31.4	32.9	15.1	17	29.9	32.8	31.3	27.2	23	7.6	31.0	53.7	30.7	31.6
Ce	35.2	33.8	66.2	16.5	55.5	87.9	59.3	64.5	31.2	33.1	58.9	68.8	60.3	54.4	50.1	12.4	64.8	99.8	61.3	66.1
Pr	4.53	4.27	7.72	2.24	7.19	10.95	7.7	8.29	4.16	4.28	6.39	8.24	7.43	6.64	6.07	1.67	7.68	11.28	6.95	6.99
Nd	17.1	15.2	28.8	8.3	26.8	40.5	29.2	31.5	16.4	17.1	20.4	29.3	26.3	23.1	22.8	5.7	28.5	38.3	26.6	25.8
Sm	3.23	2.81	5.7	1.53	4.83	6.94	5.37	6.38	3.47	3.27	3.68	5.61	4.99	4.8	4.61	1.11	5.65	6.98	5.25	4.59
Eu	0.7	0.59	1.07	0.36	0.99	1.35	1.25	1.47	0.83	0.82	0.7	1.18	1.12	1.08	0.92	0.3	1.10	1.86	0.92	1.17
Gd	2.64	2.55	5.38	1.4	3.99	5.96	5.12	6.44	3.65	3.37	3.3	5.43	4.71	4.72	4.37	0.99	4.80	5.88	4.64	3.50
Tb	0.43	0.4	0.88	0.22	0.64	0.92	0.84	1.1	0.54	0.47	0.42	0.73	0.65	0.64	0.57	0.15	0.74	0.91	0.73	0.57
Dy	2.43	2.24	5.09	1.26	3.71	4.97	4.52	5.99	3.77	3.1	2.87	5	4.6	4.29	3.94	1.07	4.38	4.94	3.87	3.37
Ho	0.53	0.51	1.07	0.26	0.74	0.95	0.94	1.25	0.81	0.67	0.54	0.93	0.94	0.87	0.78	0.21	0.80	0.91	0.84	0.76
Er	1.53	1.43	3.15	0.75	2.19	2.88	2.68	3.6	2.22	1.91	1.58	2.6	2.8	2.44	2.26	0.66	2.20	2.40	2.54	2.09
Tm	0.23	0.21	0.47	0.12	0.36	0.43	0.41	0.57	0.38	0.3	0.24	0.4	0.42	0.36	0.36	0.1	0.34	0.36	0.40	0.35
Yb	1.57	1.42	2.95	0.82	2.33	2.73	2.6	3.7	2.42	2.07	1.64	2.55	2.55	2.37	2.3	0.6	2.16	2.20	2.64	2.23
Lu	0.24	0.23	0.38	0.13	0.37	0.38	0.38	0.53	0.37	0.32	0.24	0.38	0.38	0.34	0.38	0.09	0.32	0.30	0.36	0.34
Hf	8.8	10.3	6.6	5.8	14.5	12	5.3	6.3	2.7	2.7	7.3	7	6	5.2	5.3	3.3	9.6	8.7	4.7	7.5
Ta	0.5	0.6	1.6	0.2	1	0.9	0.7	1.1	0.3	0.3	0.6	0.7	0.9	0.8	0.9	0.2	0.7	3.4	1.1	0.8
Pb	11.9	6.5	21.5	22.4	3.6	3.7	3	153.4	8	4.2	16.9	27.5	7.5	6.6	3.6	31.5	9.0	2.9	11.8	1.4
Th	5.2	6.4	8.3	2.9	11.4	18.7	10.6	7.3	4.5	4.2	8.4	15.3	13	9.1	9.8	1.3	13.1	12.1	10.4	11.0
U	1.7	1.6	3.1	1.5	2.2	2.5	2.5	1	1.6	1.4	2.3	7.2	6	2.5	2.2	0.7	1.7	1.3	2.3	1.6
W	<0.5	3.9	1	<0.5	340.9	1.4	1.2	2.8	0.7	0.9	1.1	1.8	1.5	374.2	295.2	457.4	0.8	3.3	1.3	1.7
Mo	1.1	0.4	3.8	0.3	0.2	0.2	0.6	0.8	2.5	1.2	1.2	2.1	0.4	0.4	<0.1	0.2	0.4	0.2	0.3	0.2
As	1.2	6.6	12.6	0.8	1.1	1.9	0.7	9.2	3.3	56.9	10.4	24.6	8.4	7.9	5.7	<0.5	<0.5	3.4	9.6	2.8

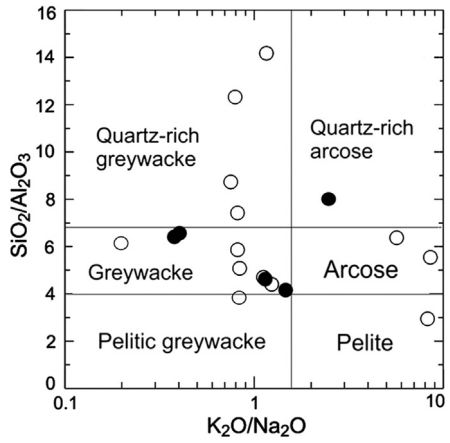

Figure 5. SiO_2/Al_2O_3 vs. K_2O/Na_2O classification plot of metasedimentary rocks of the Ghor Province (after Wimmenauer, 1984; Patočka and Štorch, 2004). Symbols: open circle – muscovite gneisses; full circle – biotite gneisses.

metabasalts, and are often predominant, especially in the Tajik block. These sedimentary rocks are characteristic of continental environment, where the clastic material of sandstones was derived from the passive continental margin and continental volcanic arc (Fig. 7C). A plausible continental environment for basalt formation is also suggested by plots in the La-Y-Nb triangle (Fig. 10).

We envisage the formation of the supracrustal sequence in a continental rifted basin, most likely of back-arc basin type. The specific geochemical patterns of back-arc basin basalts (BABB) are not well constrained, because the chemical composition of BABB lavas is influenced by a wide variety of spreading styles and lithosphere compositions, and changes in the course of the evolution of the back-arc basin. Therefore the rocks may show geochemical signatures characteristic of MORB, OIB, oceanic plateau basalts (OPB) and island arc tholeiites suggesting that the BABB might be derived from various mantle sources, ranging from depleted to enriched, and from MORB to Nb depleted, volcanic arc mantle (Poller et al., 2001; Xu et al., 2003; Ichiyama and Ischiwatari, 2004; Martinez et al., 2007).

To discriminate BABB from rocks of other tectonic settings, special diagrams are proposed. Ti and Zr concentrations (Fig. 11) demonstrate affinity of Ghor greenschists to BABB discriminating them from IAB (Woodhead et al., 1993; Poller et al., 2001). On the Ni vs. FeO^T/MgO and La/Yb vs. Nb/La diagrams discriminate BABB from OPB (Fig. 11), where Ghor samples cluster within the BABB field, partly overlapping with the OPB field (Ichiyama and Ischiwatari, 2004). The Th/Nb ratio which is comparatively low in the case of BABB is also in agreement with such a presumption. In basalts of the Lau back-arc basin this ratio ranges from 0.061 to 0.19, with an

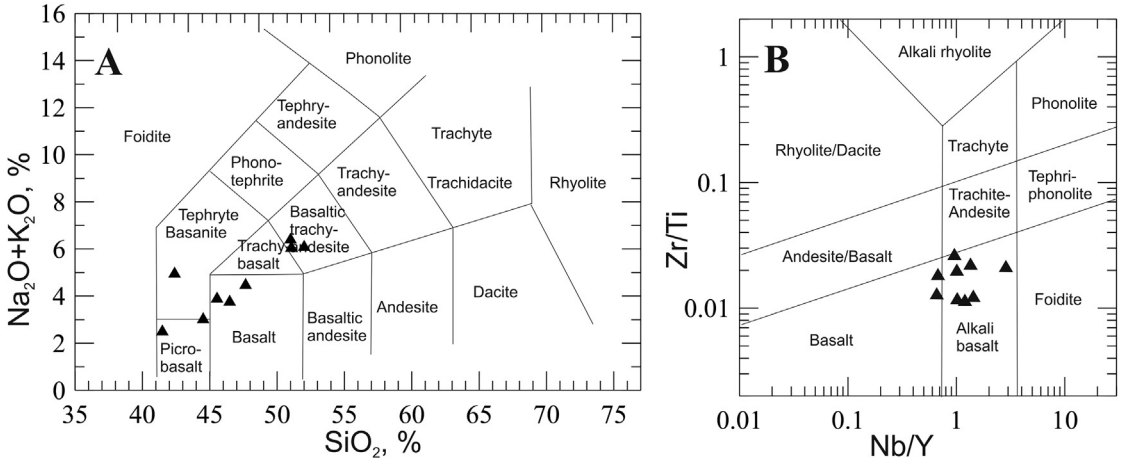

Figure 6. Classification diagrams for greenschists of the Ghor Province. (A) Total Alkali vs. SiO_2 plot (after Le Maitre, 2002); (B) Zr/Ti vs. Nb/Y plot (after Winchester and Floyd, 1977; Pearce, 1996).

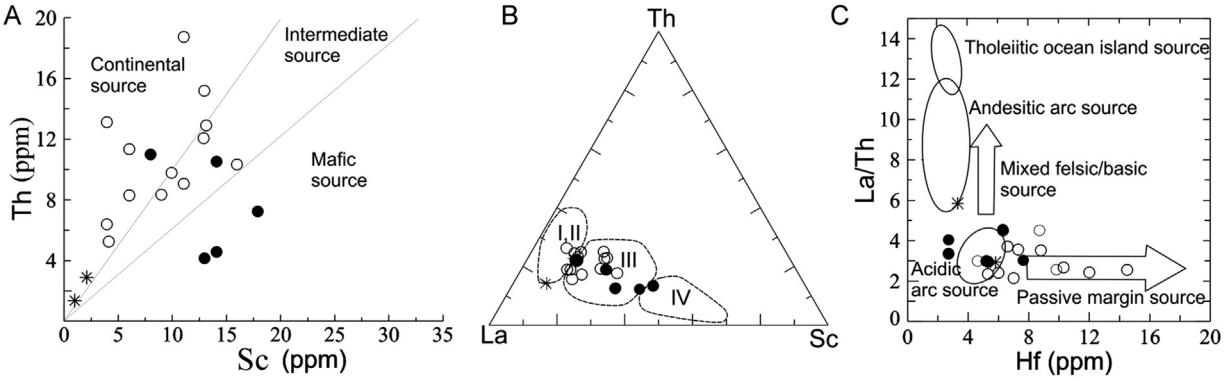

Figure 7. Discrimination diagrams of the source and tectonic setting of clastic metasedimentary rocks of the Ghor Province. (A) Th vs. Sc plot (after McLennan et al., 1993; Hinchey, 2012); (B) La-Th-Sc triplot (after Bhatia and Crook, 1986): I–passive continental margin; II – active continental margin; III–continental island arcs; IV–oceanic island arcs; (C) Hf vs. La/Th plot (after Floyd and Leveridge, 1987). Symbols: open circle–muscovite gneisses; full circle–biotite gneisses; stars–calcite bearing muscovite gneisses.

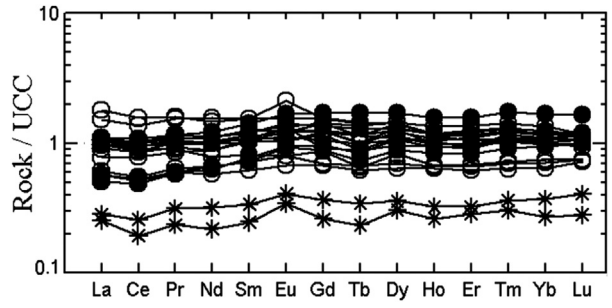

Figure 8. REE concentrations in metasedimentary rocks of the Ghor Province normalized to composition of upper continental crust (after Taylor and McLennan, 1985). Symbols as in Fig. 6.

average of 0.092 (Murray et al., 2003), while in the Ghor basalts this ratio varies from 0.09 to 0.13, except one sample (G41), where it is 0.27.

Thus, the back-arc basin tectonic setting appears to be the most plausible option, considering the geochemical patterns of basalts and those of the associated sedimentary rocks. Taking into account that provenance areas of clastic material of sediments were both passive continental margin and continental arcs, an intra-continental setting of back-arc basin might be presumed.

6.3. Implications for the recent structure of Central Ghor Province

On the geochemical diagrams, the muscovite and biotite gneisses form overlapping clusters and show common trends

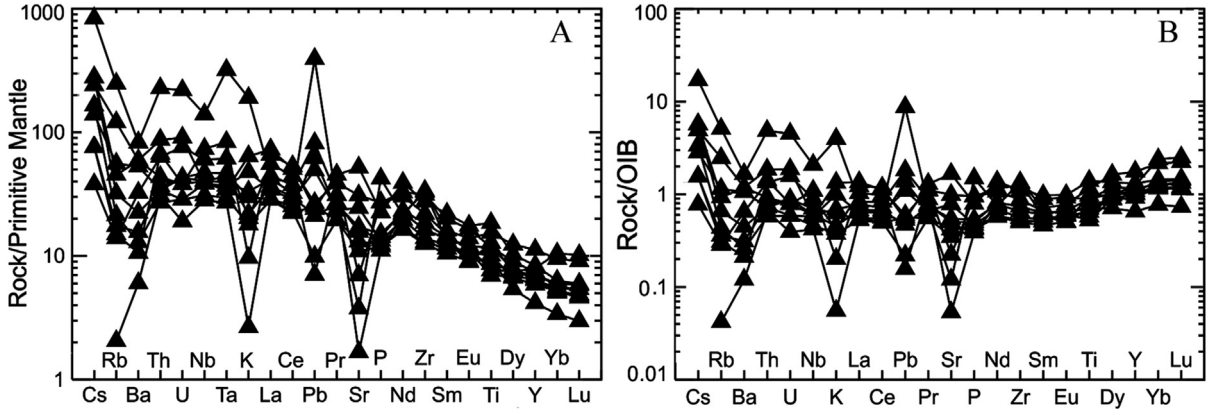

Figure 9. (A) Primitive mantle and (B) Ocean island basalt (Sun and McDonough, 1989) normalized spider diagram for greenschists of the Ghor Province.

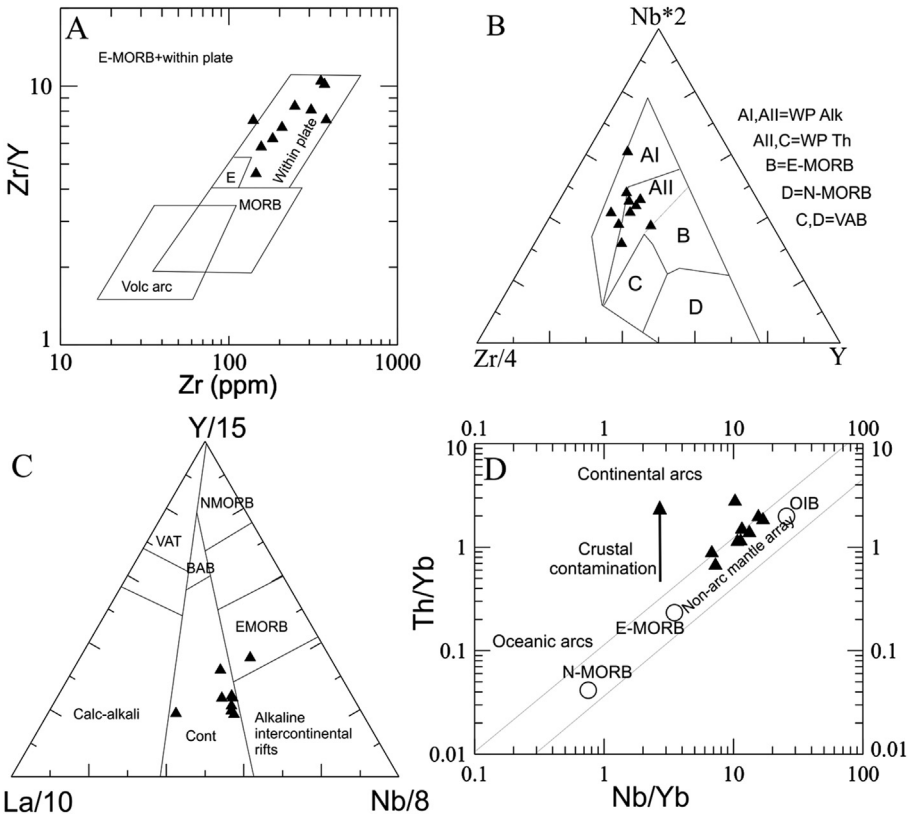

Figure 10. Diagrams for discrimination of a tectonic setting of greenschists of the Ghor Province. (A) Zr/Y vs. Zr plot (after Pearce and Norry, 1979); (B) Zr-Nb-Y triplot (after Meschede, 1986); (C) La-Y-Nb triplot (after Cabanis and Lecolle, 1989); (D) Th/Yb vs. Nb/Yb plot (after Pearce and Peate, 1995).

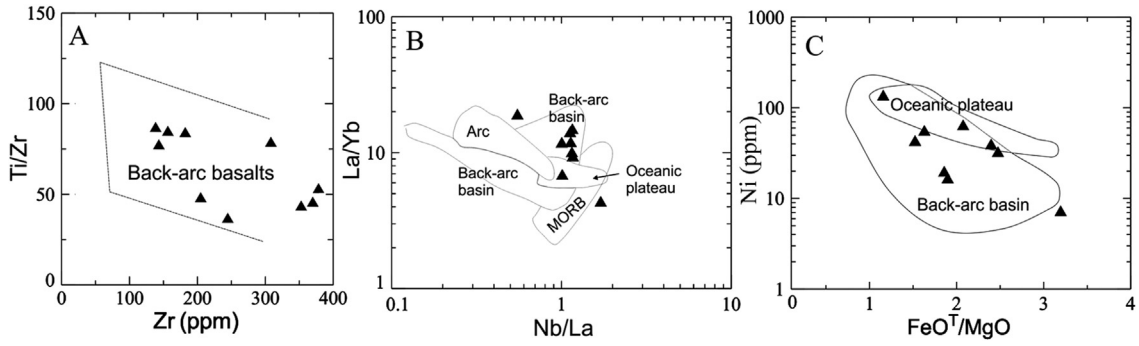

Figure 11. Diagrams for greenschists of the Ghor Province, discriminating back-arc basin basalts. (A) Ti/Zr vs. Zr plot (after Woodhead et al., 1993); (B) La/Yb vs. Nb/La plot, and (C) Ni vs. FeO^T/MgO (after Ichiyama and Ischiwatari, 2004).

suggesting the same tectonic setting of sedimentation. This implies that both lithological sequences form part of the common stratigraphic unit, the lower part of which is dominated by biotite gneisses, while muscovite gneisses comprise the upper part of the section. This presumption is supported by the higher grade of metamorphism of biotite gneisses indicating a deeper erosion level of the basement of Tajik block, where the erosion lasted up to Carboniferous, while in Band-e-Bayan zone the metamorphic rocks are covered by Ediacaran and Cambrian.

The similarities of the metamorphic rocks in both structural units support the presumption that the Band-e-Bayan zone represents the tectonized marginal part of the Tajik block.

6.4. Paleotectonic implications

The northern package presumably comprises the older part of the back-arc basin infill, whereas the southern sections comprising more metavolcanics reflect the mature stage of development of the back-arc basin (Saunders, 1986; Gracia et al., 1998).

The asymmetric basin infill can be considered as typical feature for back-arc basins of continental margin setting (Bahk and Chough, 1983; Nichols and Hall, 1991; Jean-Noël et al., 2005). According to this scenario, the terrigenous sediments were supplied from both margins, i.e., from the volcanic arc and drainage areas of the continent. Following this hypothesis, we infer that the subduction zone and associated volcanic arc were located further to the north.

According to this model, the southern part of the Tajik block and Band-e-Bayan zone represents a split margin of the originally larger continent (Gondwana supercontinent?). The rifting took place along the ancient rifted (back-arc) zone during Phanerozoic. The rift-related faults and weak zones might have been subsequently reactivated in the course of later collisional processes, in accordance to the general W–E trend of the basement lithologies that likely follows the general structural grain of the basin.

7. Conclusions

(1) The major lithologies of the Precambrian metamorphic supracrustal sequence exposed in the southern margin of the Tajik block and in the Band-e-Bayan zone are felsic gneisses (primary greywackes and arkose), greenschists (primary alkaline basalts), and marbles (primary limestones and dolomite).
(2) The interbedded supracrustal rocks form common stratigraphic sequence, the younger part of which is located in the Band-e-Bayan zone, composed of muscovite gneisses, marbles and metabasalts. The older part is in the Tajik block, represented mainly by biotite gneisses, whereas marbles and metabasalts occur in the rear domain. Correspondingly the degree of metamorphism changes from greenschist to upper amphibolites facies.
(3) The formation of the whole sequence presumably took place in continental margin rift, most probably of back-arc basin type.
(4) The Band-e-Bayan zone is a tectonized part of the Tajik continental block, sharing the same history of formation of continental crust and accretion to the Eurasian continent.
(5) The Tajik continental block, including the part of recent Band-e-Bayan zone split off from the originally larger continent (Gondwana supercontinent?) along the ancient rifted weakness (back-arc) zone during the late Paleozoic.

Acknowledgments

The present study has been carried out within the framework of the Development, Cooperation and Democracy Promotion Program coordinated by the Ministry of Foreign Affairs of the Republic of Lithuania. We are particularly thankful to the Lithuanian Provincial Reconstruction Team (PRT) in the Ghor for the organisation of the field work.

References

Abdullah, S.H., Chmyriov, V.M., 1980. Geology and Mineral Resources of Afghanistan, Book I, Geology. Nedra, Moscow, 535 pp. (in Russian).
Abdullah, S.H., Chmyriov, V.M., 1977. Geological Map of Afghanistan, Annex 1 to Geology and Mineral Resources of Afghanistan, Book I, Geology. Nedra, Moscow scale 1:2,500,000 (in Russian).
Atlas of Mineral Resources of the ESCAP Region Series, 1995. Geology and Mineral Resources of Afghanistan, vol. 11. United Nations Publication.
Bahk, K.S., Chough, S.K., 1983. Provenance of turbidites in the Ulleung (Tsushima) back-arc basin, East Sea (Sea of Japan). Journal of Sedimentary Research 53 (4), 1331–1336.
Bhatia, M.R., 1983. Plate tectonics and geochemical compositions of sandstones. Journal of Geology 91, 611–627.
Bhatia, M.R., Crook, K.A.W., 1986. Trace elements characteristics of greywackes and tectonic setting discrimination of sedimentary basins. Contributions to Mineralogy and Petrology 92, 181–193.
Cabanis, B., Lecolle, M., 1989. Le diagramme La/10-Y/15-Nb/8; un outil pour la discrimination des series volcaniques et la mise en evidence des processus de melange et/ou de contamination crustale. Comptes Rendus de l'Academie des Sciences, Serie 2, Mecanique, Physique, Chimie, Sciences de l'Univers. Sciences de la Terre 309 (20), 2023–2029 (in France with English abstract).
Dampare, S.B., Shibata, T., Asiedu, D.K., Osae, S., Banoeng-Yakubo, B., 2007. Geochemistry of paleoproterozoic metavolcanic rocks from the southern Ashanti volcanic belt, Ghana: petrogenetic and tectonic setting implications. Precambrian Research 162, 403–423.
Doebrich, J.L., Wahl, R.R., 2006. Geological and Mineral Resource Map of Afghanistan. U.S. Geological Survey Open–File Report 2006–1038, scale 1:850,000. Available on web at: http://pubs.usgs.gov/of/2006/1038/.
Dronov, V.I., Kalimulin, S.M., Sborshchikov, I.M., 1972. The Geology and Minerals of North Afghanistan. Department of Geological and Mineral Survey. Kabul, unpub. report (in Russian).
Dronov, V.I., Stazhilo–Alekseev, K.F., Kotchetkov, A.Ya, Karapetov, S.S., Kalimulin, S.M., Sonin, I.I., 1973. The Geology and Minerals of Central and

South–Western Afghanistan. Department of Geological and Mineral Survey. Kabul, unpub. report (in Russian).
Floyd, P.A., Leveridge, B.E., 1987. Tectonic Environment of the Devonian Mode and Geochemical Evidence from Turbiditic Sandstones, 144. Journal of Geological Society, London, pp. 531–542.
Gracia, E., Canals, M., Lagabrielle, Y., Auzende, J.M., 1998. Backarc evolution from rifting to mature spreading: the Bransfield and North Fiji Basins (NW Antarctica and SW Pacific). Geogaceta 20 (4), 826–829.
Hinchey, J., 2012. Preliminary insights into lithogeochemical signatures and possible provenance of reduced sedimentary units associated with copper mineralization – Western Avalon zone, Newfoundland. Current Research. Newfoundland and Labrador Department of Natural Resources Geological Survey, Report 12-1, 1–20.
Ichiyama, Y., Ischiwatari, A., 2004. Petrochemical evidence for off-ridge magmatism in a back-arc setting from the Yakuno ophiolite, Japan. Island Arc 13, 157–177.
Jean-Noël, P., Geoffroy, L., Scott, N., Peter, J.J.K., 2005. Sedimentary architecture of a Plio-Pleistocene proto-back-arc basin: Wanganui Basin, New Zealand. Sedimentary Geology 181 (3–4), 107–145.
Kalvoda, J., Bábek, O., 2010. The margins of Laurussia in central and southeast Europe and southwest Asia. Gondwana Research 17, 526–545.
Klett, T.R., Amirzada, A., Selab, A., Muty, S.A., Nakshband, H.G., Wardak, M.G., Hosine, A., Aminulah, Wahab, A., Ulmishek, G.F., Wandrey, C.J., Agena, W.F., Taylor, D.J., Hill1, R., Pribil, M., King, J.D., Pawlewicz, M.J., Barker, C.E., Ahlbrandt, T.S., Charpentier, R.R., Pollastro, R.M., Schenk, C.J., 2006. Assessment of Undiscovered Technically Recoverable Conventional Petroleum Resources of Northern Afghanistan. U.S. Geological Survey Open-File Report 1–237.
Le Maitre, R.W., 2002. Igneous Rocks: a Classification and Glossary of Terms, Recommendations of the International Union of Geological Sciences, Subcommission on the Systematics of Igneous Rocks. Cambridge University Press, Cambridge.
Martinez, F., Okino, K., Ohara, Y., Reysenbach, A.L., Gooffredi, S., 2007. Back-arc basins. Oceanography 20 (1), 116–127.
McLennan, S.M., Hemming, S., McDaniel, D.K., Hanson, G.N., 1993. Geochemical approaches to sedimentation, provenance, and tectonics. In: Johnsson, M.J., Basu, A. (Eds.), Processes Controlling the Composition of Clastic Sediments. Geological Society of America Special Papers 284, pp. 21–40.
Meschede, M.A., 1986. Method of discriminating between different types of mid-ocean basalts and continental tholeiites with the Nb-Zr-Y diagram. Chemical Geology 56, 207–218.
Murphy, B., 2007. Igneous rock associations 8. Arc magmatism II: geochemical and isotopic characteristics. Geoscience Canada 34 (1), 7–35.
Murray, C.G., Blake, P.R., Hutton, L.J., Withnall, I.W., Hayward, M.A., Simpson, G.A., Fordham, B.G., 2003. Discussion and reply. Yarrol terrane of the northern New England fold belt: forearc or backarc? Australian Journal of Earth Sciences 50, 271–293.
Nadimi, A., 2007. Evolution of the Central Iranian basement. Gondwana Research 12 (3), 324–333.
Nichols, G.J., Hall, R., 1991. Basin formation and Neogene sedimentation in a backarc setting, Halmahera, eastern Indonesia. Marine and Petroleum Geology 8 (1), 50–61.
Patočka, F., Štorch, P., 2004. Evolution of geochemistry and depositional settings of Early Palaeozoic siliciclastics of the Barrandian (Teplá-Barrandian Unit, Bohemian Massif, Czech Republic). International Journal of Earth Sciences 93, 728–741.
Pearce, J.A., Norry, M.L., 1979. Petrogenetic implications of Ti, Zr, Y, and Nb variations in volcanic rocks. Contributions to Mineralogy and Petrology 69, 33–47.
Pearce, J.A., Peate, D.W., 1995. Tectonic implications of the composition of volcanic arc magmas. Annual Review of Earth and Planetary Sciences 23, 251–285.
Pearce, J.A., 1996. A user's guide to basalt discrimination diagrams. In: Bailes, A.H., Christiansen, E.H., Galley, A.G., Jenner, G.A., Keith, J.D., Kerrich, R., Lentz, D.R., Lesher, C.M., Lucas, S.B., Ludden, J.N., Pearce, J.A., Peloquin, S.A., Stern, R.A., Stone, W.E., Syme, E.C., Swinden, H.S., Wyman, D.A. (Eds.), Trace Element Geochemistry of Volcanic Rocks; Applications for Massive Sulphide Exploration, Short Course Notes, Geological Association of Canada, 12, pp. 79–113.
In: Peters, S.G., Ludington, S.D., Orris, G.J., Sutphin, D.M., Bliss, J.D., Rytuba, J.J., (Eds.), and the U.S. Geological Survey-Afghanistan Ministry of Mines Joint Mineral Resource Assessment team, 2007. Preliminary Non-fuel Mineral Resource Assessment of Afghanistan. U.S. Geological Survey Open-File Report 2007-1214. Available on web at: http://pubs.usgs.gov/of/2007/1214/.
Poller, U., Altenberger, U., Schubert, W., 2001. Geochemical investigations of the Bergsträsser Odenwald amphibolites – implications for back-arc magmatism. Mineralogy and Petrology 72, 63–76.
von Raumer, J.F., Stampfili, G.M., Borel, G., Bussy, F., 2002. The Organization of pre-Variscan basement areas at the Gondwana margin. International Journal of Earth Sciences 91, 35–52.
Saki, A., 2010. Proto-Tethyan remnants in northwest Iran: geochemistry of the gneisses and metapelitic rocks. Gondwana Research 17 (4), 704–714.
Saunders, A.S., 1986. Geochemical Characteristics of Basaltic Volcanism within Back-arc Basins. Geological Society. Special Publications 16, London, pp. 59–76.
Şengör, A.M.C., Natal'in, B.A., 1996. Palaeotectonics of Asia: fragments of a synthesis. In: Yin, A., Harrison, M. (Eds.), The Tectonic Evolution of Asia, Rubey Colloquium. Cambridge University Press, Cambridge, pp. 486–640.
Sun, S., McDonough, W.F., 1989. Chemical and isotopic systematics of oceanic basalts: implications for mantle composition and processes. In: Saunders, A.D., Norry, M.J. (Eds.), Magmatism in the Ocean Basins. Geological Society of London, Special Publications, 42, pp. 313–345.
Taylor, S.R., McLennan, S.M., 1985. The Continental Crust: its Composition and Evolution. Blackwell, Oxford, 312 pp.
Wimmenauer, W., 1984. Das prävaristische Kristallin im Schwarzwald. Fortschritte der Mineralogie 62, 69–86 (in German with English abstract).
Winchester, J.A., Floyd, P.A., 1977. Geochemical discrimination of different magma series and their differentiation products using immobile elements. Chemical Geology 20 (4), 325–343.
Wittekindt, H., Weppert, D., 1973. Geological map of central and southern Afghanistan: German geological mission to Afghanistan. Geological Survey of the Federal Republic of Germany, scale 1:500,000.
Woodhead, J., Eggins, S., Gamble, J., 1993. High field strength and transition element systematics in island arc and back-arc basin basalts: evidence for multi-phase melt extraction and a depleted mantle wedge. Earth and Planetary Science Letters 114, 491–504.
Xu, J.F., Castillo, P.R., Chen, F.R., Niu, H.C., Yu, X.Y., Zhen, Z.P., 2003. Geochemistry of late Paleozoic mafic igneous rocks from the Kuerti area, Xinjiang, northwest China: implications for backarc mantle evolution. Chemical Geology 193, 137–154.